ISBN: 978-3-95450-232-5 ISSN: 2673-7000 doi:10.18429/JACoW-NAPAC2022-MOPA76

WAKEFIELD MODELING IN SUB-THz DIELECTRIC-LINED WAVEGUIDES*

C. Phillips†, B. Leung, X. Lu[1], P. Piot[1], Northern Illinois University, DeKalb, IL, USA
[1] also at Argonne National Laboratory, Lemont, IL, USA

Abstract

Dielectric-lined waveguides have been extensively studied to potentially support high-gradient acceleration in beam-driven dielectric wakefield acceleration (DWFA) and for beam manipulations. In this paper, we investigate the wakefield generated by a relativistic bunch passing through a dielectric waveguide with different transverse sections. We specifically consider the case of a structure consisting of two dielectric slabs, along with rectangular and square structures. Numerical simulations performed with the fine-difference time-domain of the WarpX program reveal some interesting features of the transverse wake and a possible experiment at the Argonne Wakefield Accelerator (AWA) is proposed.

INTRODUCTION

Wakefields in conventional electron accelerators are generally detrimental as they degrade the beam brightness and are possible sources of instabilities. However, wakefield can also be applied to accelerate particles with unprecedented accelerating gradients. Beam-driven wakefield accelerators could serve as building blocks for the next generation of accelerators required to support research in elementary particle physics or develop compact light sources. A relatively-simple technique to implement beam-driven wakefield acceleration is structure-based wakefield (SWFA): a high-charge "drive" electron bunch passes through a vacuum channel in a structure and produces an electromagnetic field employed to accelerate a properly delayed low-charge "main" electron bunch. A simple implementation of SWFAs consists of a dielectric-lined waveguide (often referred to as DWFA). Such an implementation has been the subject of intense research over the last three decade using cylindrical-symmetric [1, 2] and "slab" structures [3, 4].

The present research focuses on characterizing the electromagnetic-field distribution excited by a drive bunch in structures with different transverse cross sections. It is well known that the transverse section of the structure can lead to dipole-mode suppression in "slab" structures [5] but a general investigation is lacking albeit for the theoretical work reported in [6]. The numerical simulations presented in this paper will guide an experiment planned at the Argonne Wakefield Accelerator (AWA). Here, we specifically investigate the case of three structures with cross-sections

* This work was performed under the Chicagoland Accelerator Science Traineeship (CAST) program sponsored by the U.S. DOE award DE-SC0020379 to the Illinois Institute of Technology and Northern Illinois University (NIU). BL, XL, and PP are supported by DOE award DE-SC0022010 to NIU. The AWA facility is sponsored under DOE contract No. DE-AC02-06CH11357 with Argonne National Laboratory.
† z1907262@students.niu.edu

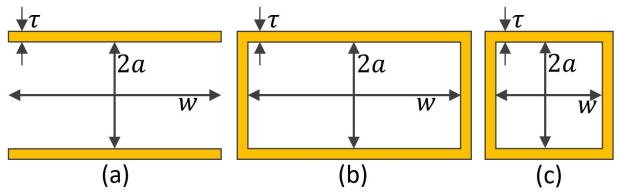

Figure 1: Cross-sectional views [in (x, y) plane] of the slab (a), rectangular (b), and square (c) structures. The structures have the same length along the z direction.

of a "slab", rectangular and square; see Fig. 1. All the considered structures are made of fused silica with the surfaces external to the beam's vacuum channel coated with a metal.

STRUCTURE MODELLING

Throughout this paper, we take the beam to propagate along the $\hat{z}$ direction with (x, y) being the transverse positions. The structures are parameterized by their vertical half gap a, full width w, and the dielectric thickness τ; see Fig. 1. The structures are translational-invariant along the $\hat{z}$ axis with axial length L. The dielectric material is assumed to be isotropic with scalar relative permittivity ϵ . The parameters considered for the present study are summarized in Table 1 and were selected based on their commercial availability. The numerical modeling was performed with WarpX – an advanced electromagnetic framework with particle-in-cell (PIC) capabilities [7]. Although WarpX is principally employed to simulate plasma wakefield accelerators, it has recently been successfully used to model the long-term dynamics in dielectric-lined waveguide [8]. Specifically, we use a fine-difference time-domain "macroscopic" electromagnetic solver. The computation domain extended from $x \in [-w/2, w/2]$, $y \in [-a, a]$, and $z \in [0, L]$. The boundary conditions at the transverse planes $z = 0$ and $z = L$ were set to perfectly-matched layers (PMLs) while all the other boundaries were configured as perfect electrical conductors (PECs) since the outer dielectric surfaces are coated with a metal. To increase simulation speed and given that only the field within and behind the bunch is of interest, a moving

Table 1: Dimensions (all in units of mm) and Relative Electric Permittivity ϵ for the Structures Displayed in Fig. 1

structure type	**2**				
slab	2	4	0.4	150	3.75
rectangular	2	4	0.4	150	3.75
square	2	2	0.4	150	3.75

ISBN: 978-3-95450-232-5 ISSN: 2673-7000 doi:10.18429/JACoW-NAPAC2022-MOPA76

Table 2: Wakefield Excited in the Three Structures Shown in Fig. 1 by a 2-nC Bunch

structure type	frequency (GHz)	peak field (MV/m)
slab	62.75	20.19
rectangular	50.20	21.62
square	100.39	30.19

window co-propagating with the beam is employed. Convergence studies were performed and ultimately the mesh size was set $64 \times 64 \times 256$. The three different structures depicted in Fig. 1 were modeled and the fundamental frequency and peak fields are summarized in Table 2. The fundamental frequency was extracted from a Fast-Fourier-Transform analysis of the axial $E_z(x = y = 0, z, t)$. The model uses a bunch of 800k macroparticles initialized to follow Gaussian distributions along all degrees of freedom. The fields are initialized and applied to the macroparticle at $z = 10\,\text{mm}$ using WARPX's "plane injection" method. The corresponding axial electric fields appear in Fig. 2. For these simulations the input-beam distribution was taken to have RMS transverse and longitudinal beam sizes of respectively $\sigma_x = \sigma_y = 50\,\mu\text{m}$, and $\sigma_z = 200\,\mu\text{m}$. The bunch charge and energy are respectively taken to $Q = 2\,\text{nC}$, and $\mathcal{E} = 40\,\text{MeV}$. The field maximum field amplitudes are on the order of $\sim 20\,\text{M/m}$ for all the rectangular and slab structures and 50% higher for the square structure. It should be noted that in the present simulation the slab is assumed to have conducting wall (PEC-boundary conditions) at $x = \pm w/2$.

A critical aspect of our studies is to explore the transverse-wake structure. Figure 3 presents the transverse field $\mathbf{F}_\perp = [\mathbf{E} + c\hat{\mathbf{z}} \times \mathbf{B}]_\perp$ computed from the electromagnetic field

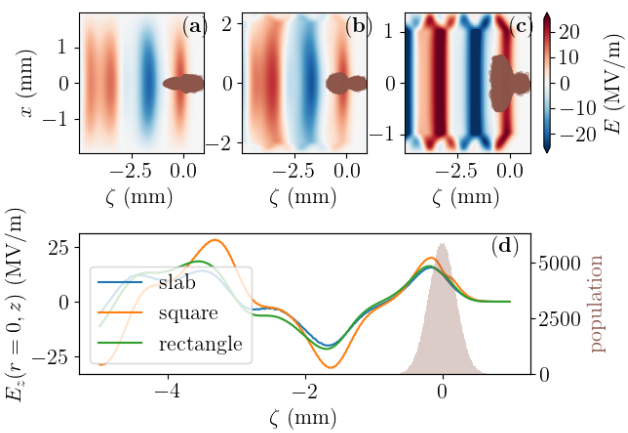

Figure 2: Axial electric field $E_z(x = 0, y, z)$ in the symmetry plane of the structures ($x = 0$) for the slab (a), rectangular (b) and square (c) structure and comparison of the axial field $E_z(x = y = 0, z)$ (d). The longitudinal coordinate $\zeta \equiv z - \bar{z}$ is defined with respected to the bunch center $\bar{z}$. The red points in (a-c) represent the macroparticle positions in (z, x).

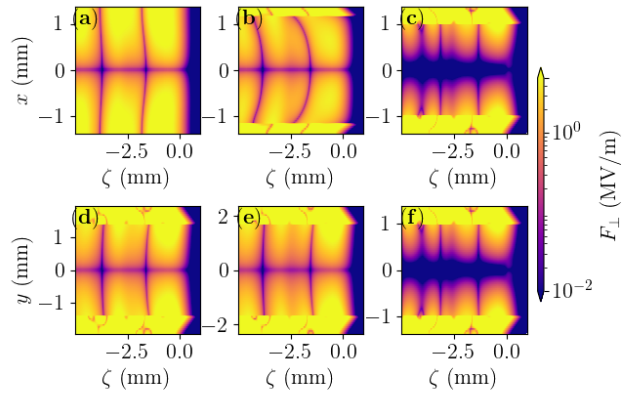

Figure 3: Modulus of the transverse field $|\mathbf{F}_\perp|$ computed in the $y = 0$ (a-c) and $x = 0$ (d,e) symmetry planes of the computational domain for the slab (a,c), rectangular (b,d) and square (c,e) structures.

$\{\mathbf{E}, \mathbf{B}\}(x, y, z)$ at the final time step of the simulation. The simulated transverse force exhibits some intricate structures which especially indicates the force vanishes at several locations in addition to the center of the structure $(x, y) = (0, 0)$. To further examine this feature we show in Fig. 4 the force computed in transverse slices $|\mathbf{F}_\perp(x, y)|$. We show the force computed at the same distance $\zeta \simeq -2.1\,\text{mm}$ (this choice is just a convenience and it should be noted that the spatial frequency of the transverse wakefield is different for the three structures). For the slab and rectangular structures, the transverse force cancels at three points (or "vertices") arranged along the $y = 0$ axis. As the axial position of the observation plan is varied the transverse separation between these vertices changes and, ultimately, the vertices collapse to the point $(x, y) = (0, 0)$ point. The square structure does not display such intricate structures. The presence of several loci with vanishing transverse force in asymmetric structures could be taken advantage of to control the transverse wakefield [9].

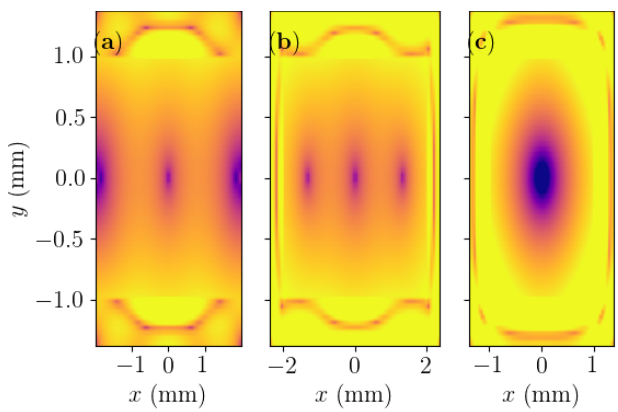

Figure 4: Modulus of the transverse field $|\mathbf{F}_\perp(x, y)|$ computed in a transverse plane at $\zeta \simeq -2.1\,\text{mm}$ for the slab (a), rectangular (b) and square (c) structures. The color map used is identical to the one in Fig. 3.

ISBN: 978-3-95450-232-5 ISSN: 2673-7000 doi:10.18429/JACoW-NAPAC2022-MOPA76

PROPOSED EXPERIMENT AT AWA

An experiment to investigate the transverse structure of the wakefield produced in the three structures discussed above is in preparation at AWA. The AWA beamline incorporates a photoinjector capable of producing high-charge electron bunches with energies up to ~ 60 MeV. The bunch will be transported to the interaction chamber, located 28-m from the photocathode, where the structures will be installed on a movable insertion device. Previous beam-dynamics studies indicate that a 1 nC bunch can be focused to sub-μm transverse size. Downstream of the structure, a single-shot longitudinal phase space (LPS) diagnostic is available. The beamline consists of quadrupoles, a transverse deflecting cavity (streaking the beam in the vertical direction), and a horizontal dipole magnet followed by a spectrometer. This beamline allows for the time-energy distribution to be mapped in the (x, y) plane and directly observable on a standard YAG screen [10].

A simple matrix-based model was implemented in PYTHON to simulate the LPS measurement system of the AWA beamline. This script can be used to find the optimal quadrupole-magnet settings to create a beam waist at the end of the measurement system and ensure the mapping of the LPS (ζ, δ) coordinates in the (x, y) plane is optimized. The program is also used to track the beam distribution through the LPS-diagnostic beamline. An example of simulation for the case of the rectangular structure appears in Fig. 5. The simulation so far confirms that the system can properly resolve the longitudinal wakefield [as inferred by comparing Fig. 5(b) and (c)] and can also provide spatiotemporal distribution, e.g., (ζ, x); see Fig. 5(a,c).

The LPS-diagnostic simulations confirm that the available beamline has sufficient resolution to resolve the beam distortions (energy loss and time-dependent energy loss and focusing). However, developing a technique to resolve the structure of the wakefield behind the bunch is underway. Several methods are being considered including the use of multiple witness bunches configured as a patterned beam as previously investigated in [11, 12].

CONCLUSION

We have performed WARPX simulations for several configurations of dielectric-lined waveguides aimed at exploring the transverse structure of the wakefield driven by a high-charge bunch. These simulations were coupled to a simple model of the diagnostic beamline to investigate possible experimental signatures. These simulations provide confidence in the feasibility of an experiment at AWA. Refined simulations coupling WARPX to a beam-dynamics program (OCELOT or OPAL-T) will be performed to finalize the experimental plan including the possible generation and diagnosis of a witness bunch to sample the wakefield structure.

ACKNOWLEDGMENTS

We thank Wei Hou Tan (NIU) for sharing his implementation of dielectric boundaries in WARPX used in [8].

This research used the open-source particle-in-cell code WARPX, https://github.com/ECP-WarpX/WarpX, primarily funded by the US DOE Exascale Computing Project. Primary WARPX contributors are with LBNL, LLNL, CEA-LIDYL, SLAC, DESY, CERN, and Modern Electron. We acknowledge all WARPX contributors.

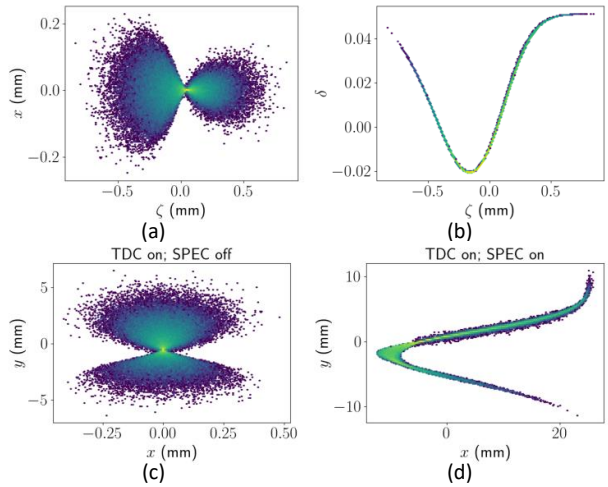

Figure 5: Simulation of the LPS measurement diagnostics for the case of the rectangular structure. The upper plots give the initial (ζ, x) spatiotemporal (a) and LPS (b) distributions. The lower plots present the simulated distribution downstream of TDC only (c) and TDC and dipole magnet (d).

REFERENCES

[1] W. Gai *et al.*, "Experimental demonstration of wake-field effects in dielectric structures," *Phys. Rev. Lett.*, vol. 61, pp. 2756–2758, 1988. doi:10.1103/PhysRevLett.61.2756

[2] B. D. O'Shea *et al.*, "Observation of acceleration and deceleration in gigaelectron-volt-per-metre gradient dielectric wakefield accelerators," *Nature Communications*, vol. 7, no. 1, p. 12 763, 2016. doi:10.1038/ncomms12763

[3] A. Tremaine, J. Rosenzweig, and P. Schoessow, "Electromagnetic wake fields and beam stability in slab-symmetric dielectric structures," *Phys. Rev. E*, vol. 56, pp. 7204–7216, 1997. doi:10.1103/PhysRevE.56.7204

[4] D. Mihalcea, P. Piot, and P. Stoltz, "Three-dimensional analysis of wakefields generated by flat electron beams in planar dielectric-loaded structures," *Phys. Rev. ST Accel. Beams*, vol. 15, p. 081 304, 2012. doi:10.1103/PhysRevSTAB.15.081304

[5] B. D. O'Shea *et al.*, "Suppression of deflecting forces in planar-symmetric dielectric wakefield accelerating structures with elliptical bunches," *Phys. Rev. Lett.*, vol. 124, p. 104 801, 2020. doi:10.1103/PhysRevLett.124.104801

[6] S. S. Baturin and A. D. Kanareykin, "New method of calculating the wakefields of a point charge in a waveguide of arbitrary cross section," *Phys. Rev. Accel. Beams*, vol. 19, p. 051 001, 2016. doi:10.1103/PhysRevAccelBeams.19.051001

ISBN: 978-3-95450-232-5 ISSN: 2673-7000 doi:10.18429/JACoW-NAPAC2022-MOPA76

[7] A. Myers *et al.*, "Porting WarpX to GPU-accelerated platforms," *Parallel Computing*, vol. 108, p. 102 833, 2021. doi:https://doi.org/10.1016/j.parco.2021.102833

[8] W. Tan *et al.*, "Simulation Studies of Drive Beam Instability in a Dielectric Wakefield Accelerator," in *Proc. IPAC'22*, Bangkok, Thailand, 2022, paper MOPOMS012, pp. 645–648. doi:10.18429/JACoW-IPAC2022-MOPOMS012

[9] S. S. Baturin, G. Andonian, and J. B. Rosenzweig, "Analytical treatment of the wakefields driven by transversely shaped beams in a planar slow-wave structure," *Phys. Rev. Accel. Beams*, vol. 21, p. 121 302, 2018. doi:10.1103/PhysRevAccelBeams.21.121302

[10] Q. Gao *et al.*, "Single-shot wakefield measurement system," *Phys. Rev. Accel. Beams*, vol. 21, p. 062 801, 2018. doi:10.1103/PhysRevAccelBeams.21.062801

[11] A. Halavanau *et al.*, "Spatial control of photoemitted electron beams using a microlens-array transverse-shaping technique," *Phys. Rev. Accel. Beams*, vol. 20, p. 103 404, 2017. doi:10.1103/PhysRevAccelBeams.20.103404

[12] A. Halavanau, Y. Ding, C. E. Mayes, P. Piot, and S. Baturin, "Hollow Electron Beams in a Photoinjector," in *Proc. IPAC'20*, Caen, France, 2021, p. 49. doi:10.18429/JACoW-IPAC2020-WEVIR06